HHS Public Access

Author manuscript

Cell Host Microbe. Author manuscript; available in PMC 2017 June 09.

Published in final edited form as:

Cell Host Microbe. 2016 August 10; 20(2): 215–225. doi:10.1016/j.chom.2016.07.006.

Fap2 Mediates *Fusobacterium nucleatum* Colorectal Adenocarcinoma Enrichment by Binding to Tumor-Expressed Gal-GalNAc

Jawad Abed[1,9], **Johanna E.M. Emgård**[1,9], **Gideon Zamir**[2], **Mouhammad Faroja**[2], **Gideon Almogy**[2], **Amalie Grenov**[1], **Asaf Sol**[1], **Ronit Naor**[1], **Eli Pikarsky**[3,4], **Karine A. Atlan**[4], **Anna Mellul**[4], **Stella Chaushu**[5], **Abigail L. Manson**[6], **Ashlee M. Earl**[6], **Nora Ou**[7], **Caitlin A. Brennan**[7], **Wendy S. Garrett**[6,7,8,10,*], and **Gilad Bachrach**[1,10,*]

[1]The Institute of Dental Sciences, The Hebrew University-Hadassah School of Dental Medicine, Jerusalem 91120, Israel

[2]Department of General Surgery, Hadassah-Hebrew University Medical Center, Jerusalem 91120, Israel

[3]Department of Immunology and Cancer Research, Institute for Medical Research Israel Canada, Hebrew University-Hadassah Medical School, Jerusalem 91120, Israel

[4]Department of Pathology, Hadassah-Hebrew University Medical Center, Jerusalem 91120, Israel

[5]Department of Orthodontics, The Hebrew University-Hadassah School of Dental Medicine, Jerusalem 91120, Israel

[6]Broad Institute of MIT and Harvard University, Cambridge, MA 02141, USA

[7]Departments of Immunology and Infectious Diseases and Genetics and Complex Diseases, Harvard T.H. Chan School of Public Health, Boston, MA 02115, USA

[8]Department of Medical Oncology, Dana-Farber Cancer Institute, Boston, MA 02115, USA

SUMMARY

Fusobacterium nucleatum is associated with colorectal cancer and promotes colonic tumor formation in preclinical models. However, fusobacteria are core members of the human oral microbiome and less prevalent in the healthy gut, raising questions about how fusobacteria localize to CRC. We identify a host polysaccharide and fusobacterial lectin that explicates fusobacteria abundance in CRC. Gal-Gal-NAc, which is overexpressed in CRC, is recognized by fusobacterial

[*]Correspondence: wgarrett@hsph.harvard.edu (W.S.G.), giladba@ekmd.huji.ac.il (G.B.) http://dx.doi.org/10.1016/j.chom.2016.07.006.

[9]Co-first author

[10]Co-senior author

SUPPLEMENTAL INFORMATION

Supplemental Information includes Supplemental Experimental Procedures, three figures, and one table and can be found with this article online at http://dx.doi.org/10.1016/j.chom.2016.07.006.

AUTHOR CONTRIBUTIONS

J.A., W.S.G., and G.B. designed the experiments, analyzed the data, and wrote the paper. J.A., J.E.M.M., G.Z., M.F., G.A., A.G., A.S., R.N., E.P., K.A.A., A.M., S.C., N.O., and C.A.B. carried out experiments and/or facilitated access to clinical samples. A.L.M., A.M.E., and C.A.B. carried out genomic analyses.

Fap2, which functions as a Gal-Gal-NAc lectin. *F. nucleatum* binding to clinical adenocarcinomas correlates with Gal-GalNAc expression and is reduced upon O-glycanase treatment. Clinical fusobacteria strains naturally lacking Fap2 or inactivated Fap2 mutants show reduced binding to Gal-GalNAc-expressing CRC cells and established CRCs in mice. Additionally, intravenously injected *F. nucleatum* localizes to mouse tumor tissues in a Fap2-dependent manner, suggesting that fusobacteria use a hematogenous route to reach colon adenocarcinomas. Thus, targeting *F. nucleatum* Fap2 or host epithelial Gal-GalNAc may reduce fusobacteria potentiation of CRC.

Graphical abstract

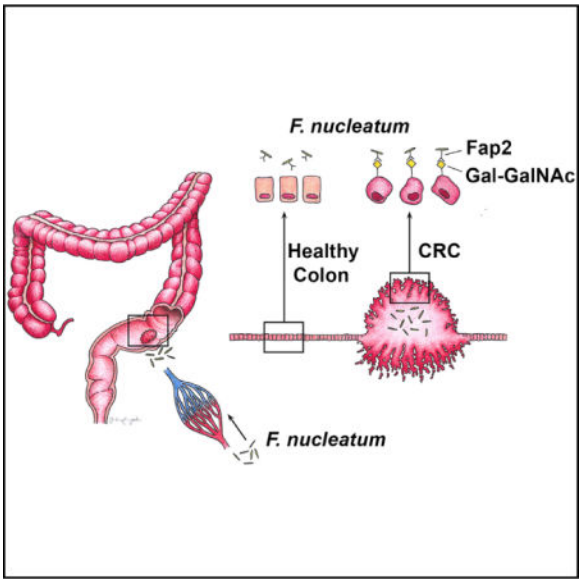

INTRODUCTION

Colorectal cancer (CRC) is the third leading cause of cancer-related deaths in the United States (Siegel et al., 2015), and microbes have emerged as key factors that influence the development, progression, and response to treatment of CRC (Garrett, 2015; Sears and Garrett, 2014; Thomas and Jobin, 2015). Enterotoxigenic *Bacteroides fragilis* accelerates colon tumor development by inducing an acute and self-limited colitis triggering an Il-23 and Il-17 inflammatory response in intestinal ad-enoma-prone $Apc^{Min/+}$ mice (Wu et al., 2009). Colibactin-expressing *Escherichia coli* potentiates colorectal carcinogenesis in azoxymethane-exposed gnotobiotic $Il10^{-/-}$ mice (Arthur et al., 2012). In addition, carbohydrate-derived bacterial metabolites, such as butyrate, can increase hyperproliferation in $Msh2^{-/-}$ (DNA mismatch repair gene *Mut*S homolog 2) colon epithelial cells, in contrast with the ingestion of a low-fiber diet that reduces tumor numbers in $Apc^{Min/+}Msh2^{-/-}$ mice (Belcheva et al., 2014). These data reflect a spectrum of ways by which bacteria contribute to colorectal carcinogenesis.

Recent metagenomic and transcriptomic analyses have revealed an enrichment of *Fusobacterium* species in human CRCs and adenomas compared with adjacent normal tissue (Castellarin et al., 2012; Chen et al., 2012; Flanagan et al., 2014; Ito et al., 2015; Kostic et

al., 2012; McCoy et al., 2013). Increased levels of *F. nucleatum* correlate with specific molecular subsets of CRCs such as the CpG island methylator phenotype and microsatellite instability (Mima et al., 2015; Tahara et al., 2014). *F. nucleatum* accelerates CRC in preclinical models using both in vitro and in vivo systems (Kostic et al., 2013; Rubinstein et al., 2013). *F. nucleatum* also suppresses anti-tumor immunity and inhibits tumor killing by natural killer (NK) cells (Gur et al., 2015). All of these findings support that *F. nucleatum* not only localizes to and is enriched in colon adenomas and colorectal adenocarcinoma but also may function in tumor growth and survival.

However, the mechanism underlying fusobacteria localization to and enrichment in CRC and colonic adenomas has been unclear from previous reports (Castellarin et al., 2012; Kostic et al., 2012, 2013; Rubinstein et al., 2013). We identify a host factor D-galactose-β(1–3)-N-acetyl-D-galactosamine (Gal-GalNAc) and a microbial protein, Fap2, that explicates fusobacterial enrichment in CRC. Herein, we show that Fap2 plays a critical role in mediating fusobacterial CRC enrichment by binding to the carbohydrate moiety Gal-GalNAc, which is overexpressed in human colorectal adenocarcinoma and metastases.

RESULTS

F. nucleatum Attaches to Gal-GalNAc Overexpressed on CRC

Binding of *F. nucleatum* to some bacterial and mammalian cells can be inhibited with sugars containing D-galactose or Gal-GalNAc (Kolenbrander and Andersen, 1989; Mongiello and Falkler, 1979; Ozaki et al., 1990). Gal-GalNAc can also be expressed at high levels by adenocarcinomas (Giannasca et al., 1996; Sakuma et al., 2015; Springer, 1984; Yang and Shamsuddin, 1996). These observations led to the hypothesis that colorectal adenocarcinoma expression of Gal-GalNAc may facilitate binding of fusobacteria to CRC. To test this hypothesis, we assessed Gal-GalNAc levels on healthy human colorectal tissues, human colonic adenomas, and human colorectal adenocarcinomas by staining tissue microarrays with fluorescein isothiocyanate (FITC)-labeled peanut agglutinin (PNA), a Gal-GalNAc [Gal - β (1→3)GalNAc] specific lectin. Gal-GalNAc levels were significantly higher in adenocarcinomas compared with adenomas (Figures 1A and 1B). Intense staining was detected in the adenocarcinoma's epithelial cells, with some variation of staining intensity across tumoral epithelial cells due to plane of section (Figure 1A). Although adenomas overall seemed to express levels of Gal-GalNAc similar to healthy tissues (Figures 1A and 1B), when we considered the histopathology of the adenomas in more detail, statistically significant trends emerged within the adenoma group. Within our data set, the highest levels of Gal-GalNAc expression were found on villous adenomas, followed by tubulous villous adenomas (14-fold difference, $p < 0.0001$, ANOVA, Tukey's multiple comparison test). Gal-GalNAc differed by 100-fold between villous and tubular adenomas ($p < 0.0001$, ANOVA, Tukey's multiple comparison test). Levels of Gal-GalNAc staining were markedly lower on adenomatoid, hyperplastic, and serrated adenomas (Figure 1C). Notably, of these histopathologic subtypes, the villous growth pattern of adenomas has the highest malignant potential.

To determine if colorectal adenocarcinoma Gal-GalNAc levels may affect *F. nucleatum* enrichment, we tested if O-glycanase reduced Gal-GalNAc levels in human colorectal

adenocarcinoma tissue sections. O-glycanase treatment of the human CRC adenocarcinoma sections reduced FITC-PNA staining by nearly 7-fold (Figures 2A and 2B). Next, we developed a method to visualize binding of *F. nucleatum* ATCC 23726 (*Fn*) to formalin-fixed paraffin-embedded human adenocarcinoma samples (Figure 2C). *Fn* binding to adenocarcinoma versus normal colonic tissues correlated with Gal-GalNAc expression levels and increased 6.1-fold in the colonic adenocarcinoma tissues relative to normal tissue ($p < 0.0001$; Figures 2C–2E). Similar to the observations with O-glycanase treatment and FITC-PNA binding, fusobacterial attachment to the colorectal adenocarcinoma specimens decreased in O-glycanase-treated sections (2.96-fold less, $p = 0.0313$; Figure 2E).

Fap2 Mediates Attachment of *F. nucleatum* to Gal-GalNAc Overexpressed in CRC

Many strains of *F. nucleatum* (approximately 80%) adhere to human erythrocytes. In most of these strains, this binding is strongly inhibited by galactose and GalNAc (Tuttle et al., 1992). The Fap2 surface protein of *F. nucleatum* ATCC 23726 is a galactose-binding lectin that mediates fusobacterial hemagglutination. Fap2 was identified by screening a *F. nucleatum* ATCC 23726 transposon mutant library for clones unable to hemagglutinate. The selected non-hemagglutinating mutants K50 and D22 both harbored the transposon in their *fap2* gene (Coppenhagen-Glazer et al., 2015). Because Fap2 mediates galactose-sensitive fusobacterial binding to erythrocytes, we hypothesized that Fap2 might also mediate binding of *F. nucleatum* ATCC 23726 to tumors that overexpress Gal-GalNAc. To test this hypothesis, we performed hemagglutination assays in the presence or absence of GalNAc using WT *Fn* and two Fap2-inactivated mutants, K50 and D22 (Figure 3A). These hemagglutination data suggest that Fap2 mediates Gal-GalNAc binding by fusobacteria. Next, we found that GalNAc inhibits binding of *F. nucleatum* ATCC 23726 to human CRC tissue sections (Figures 3B and 3C). Both Fap2-inactivated mutants K50 and D22 display impaired attachment to human colon adenocarcinoma sections compared with the wild-type *F. nucleatum* ATCC 23726 parental strain, with a mean overall reduction in abundance of 2.8- and 3.1-fold, respectively (Figures 3D–3G). Similar to PNA binding (Figure 1B), attachment of *F. nucleatum* ATCC 23726 to adenoma sections overall is not different from binding to normal colon tissues, nor is it different from K50 mutant binding (Figure 3E). In addition, fluorescence microscopy analysis of human CRC sections demonstrates co-localization (81.6%) of FITC-labeled Fap2-expressing *F. nucleatum* ATCC 23726 with tumor Gal-GalNAc detected in tumor sections from three individuals (visualized with Alexa Fluor 647-conjugated PNA and FITC-labeled *F. nucleatum* ATCC 23726) (Figure 3H). These data support that *F. nucleatum* Fap2 and tumor-expressed Gal-GalNAc play an important role in *F. nucleatum* CRC enrichment and localization.

To confirm that fusobacterial attachment to CRC is Gal-GalNAc mediated, we used both flow cytometry and competition assays. Flow cytometry analysis of the attachment of FITC-labeled *F. nucleatum* ATCC 23726 to human and mouse CRC cell lines revealed a correlation between bacterial attachment and cell line Gal-GalNAc expression levels measured using FITC-labeled PNA. Human HCT116 colon carcinoma cells, which expressed the highest amounts of Gal-GalNAc (mean 87.7% of cells binding PNA above threshold; Figure 4A), bind the highest amounts of fusobacteria (mean 87.9% of cells binding above threshold; Figure 4A). Mouse CT26 and human RKO CRC cells, expressing

intermediate levels of Gal-GalNAc (means 74.6% and 72.1%, respectively), bind intermediate amounts of *F. nucleatum* ATCC 23726 (means 71.8% and 64.8%, respectively; Figure 4A). Human HT29 CRC cells that express low levels of Gal-GalNAc (mean 1.43%) demonstrate lower (mean 18.6%) fusobacterial attachment levels. Furthermore, binding of *F. nucleatum* ATCC 23726 to the high and intermediate Gal-GalNAc-expressing cell lines is inhibited by GalNAc in a statisticallysignificant, dose-dependentmanner (p= 0.04167; Figure4A). These findings corroborate the importance of the Gal-GalNAc moiety for the attachment of the fusobacteria we evaluated. In agreement with the results demonstrating the role of Fap2 in fusobacterial attachment to CRC sections (Figures 3D–3G), both Fap2-inactivated *F. nucleatum* ATCC 23726 mutants K50 and D22 have significantly impaired attachment to the high and intermediate Gal-GalNAc-expressing CRC cell lines, compared with the wild-type parental strain ($p < 0.01$; Figure 4A). The residual binding of K50 and D22 to the CRC cells is not GalNAc sensitive, confirming the role of Fap2 in Gal-GalNAc-mediated *F. nucleatum* ATCC 23726 CRC attachment. This residual binding may be FadA-mediated (Coppenhagen-Glazer et al., 2015; Han et al., 2005). Binding of both Fap2 mutants to the HCT116 cells is higher than to the other tested cells suggesting that this cell line may express additional fusobacterial-binding ligands.

We also tested if Gal-GalNAc mediates CRC-binding by *F. nucleatum* strains CTI-2 and CTI-7, which were isolated from human CRC samples (Gur et al., 2015). Although CTI-2 possesses the *fap2* gene and its hemagglutination is inhibited by GalNAc, *fap2* is not found in CTI-7's genome and CTI-7 does not hemagglutinate (Figure S1). Although both strains bind the low Gal-GalNAc-expressing HT-29 CRC cells in a similar manner, binding of CTI-2 to the high and intermediate Gal-GalNAc-expressing HCT116, CT26, and RKO CRC cells is significantly higher than that of the non-hemagglutinating, naturally Fap2-deficient CTI-7 ($p < 0.01$; Figure 4B). Binding of CTI-2 to the high and intermediate Gal-GalNAc-expressing CRC cells is inhibited by the addition of soluble GalNAc in a dose-dependent manner ($p = 0.04167$; Figure 4B), but binding of the Fap2-deficient CTI-7 is not (Figure 4B). Correlation between Fap2 expression (detected by hemagglutination; Figure S1) and attachment to GalNAc-expressing CRC cell lines is also observed in four additional CRC *F. nucleatum* isolates, two *F. nucleatum* oral strains, and one *F. nucleatum* strain isolated from a patient with inflammatory bowel disease (Figure 4C).

Blood-Borne *F. nucleatum* Preferentially Colonizes Colorectal Tumors

We hypothesized that fusobacteria that colonize CRC originate from the oral cavity, as fusobacteria are core resident members of the human oral microbiome and are found infrequently in the gut (Human Microbiome Project Consortium, 2012; Dewhirst et al., 2010; Faust et al., 2012; Strauss et al., 2011). Previously in $Apc^{Min/+}$ mice, we observed that oral daily inoculation of fusobacteria enhanced adenoma development in the large intestine and that fusobacteria are detectable in these tumor by qPCR and fluorescence in situ hybridization (Kostic et al., 2013). Transient bacteremia is common during periodontal disease with bacterial loads reaching 10^4 bacteria/ml blood 15 min after tooth brushing in humans (Ashare et al., 2009). Thus, transient bacteremia enables access of oral fusobacteria to the circulatory system. To test whether blood-borne fusobacteria can localize to CRC, we used the orthotopic rectal CT26 adenocarcinoma model (Kolodkin-Gal et al., 2009) (Figure

5A). We injected CT26 cells stably transfected with the luciferase (*luc*) gene (CT26-luc) under the mucosa of the distal rectum of BALB/cJ wild-type mice and assessed tumor volume and spread both by real-time imaging of luciferase expression and by direct measurement of rectal tumors. Once tumor volumes reached 2,500 mm^3, mice were randomized to a control group or inoculated with 5×10^6 to 1×10^7 *F. nucleatum* ATCC 23726 by tail vein injection. Tumors and adjacent non-cancerous colon samples were harvested 24 hr post-inoculation. Consistent with the samples from human colon adenocarcinoma, Gal-GalNAc (measured using FITC-labeled PNA) is overexpressed in the mouse CRC sections compared with sections prepared from adjacent normal colon tissues (Figures 5B and 5C). In agreement with prior work in mouse models and humans (Kostic et al., 2012, 2013), the abundance of fusobacteria in tumor tissues is significantly higher than in adjacent normal tissues both by plating and qPCR ($p = 0.0005$ and $p = 0.0117$, respectively; Figures 5D and 5E). Also, intravenously inoculated fusobacteria are not found in the colons of control mice without CRC (Figures 5D and 5E), suggesting that the presence of dysplastic or neoplastic lesions assists or is required for colonic localization of blood-borne fusobacteria. We also performed tail vein injection of fusobacteria in $Apc^{Min/+}$ mice. In these experiments, we injected mice after the 12th week of age to ensure that the mice would have ample numbers of small intestinal adenomas. In our mouse facility, we very rarely observe colonic adenomas of $Apc^{Min/+}$ mice without fusobacterial inoculation. Twenty-four hours after injection, we detect wild-type *F. nucleatum* ATCC 23726 in small intestinal tissues from C57BL/6 $Apc^{Min/+}$ mice by qPCR in 11 of 12 samples (91.7%) and 0 of 6 samples from C57BL/6 wild-type mice (Table S1). When we injected C57BL/6 $Apc^{Min/+}$ and wild-type mice with K50, *F. nucleatum* is detected in 9 of 16 (56%) and 0 of 6 samples, respectively. Thus, colonization of the Fap2-expressing wild-type strain (91.7%) is significantly higher than that of K50 (9 of 16 [56%]) ($p = 0.022$, Mann-Whitney U test) (Table S1). These data indicate that Fap2 plays a role in *F. nucleatum* tumor enrichment in this model; however, the small intestinal localization of these tumors as well as the fact that $Apc^{Min/+}$ adenoma histology does not fully recapitulate the spectrum of human colonic adenoma histology complicates interpretation and application to humans.

Tumor colonization does not appear to be a general feature of oral anaerobic bacteria associated with periodontitis. *Porphyromonas gingivalis*, is an oral Gram-negative, anaerobic periodontal bacterium (Hajishengallis et al., 2011) that was previously found to be overabundant in gingival squamous cell carcinoma (Gao et al., 2016; Katz et al., 2011; Whitmore and Lamont, 2014). When mice were intravenously inoculated with *P. gingivalis*, its levels in tumors are below the limit of detection both by culturing (~10 CFU/gr tissue) and qPCR (Figures 5D and 5E). Thus, *F. nucleatum* likely harbors distinctive features that underpin its tumor localization, such as Fap2 the focus of this work and FadA (Rubinstein et al., 2013).

Fap2 Mediates CRC Colonization by *F. nucleatum* in the CT26 CRC Model

We also used the orthotopic CT26 CRC model to evaluate the role of Fap2 in CRC localization by fusobacteria. Mice were inoculated with wild-type (Fap2-expressing) *F. nucleatum* ATCC 23726 or with the Fap2-inactivated mutant D22. CRC colonization by the Fap2-deficient mutant D22 is significantly lower than that of the Fap2 sufficient ATCC

23726 parental strain as determined both by colony counting (45.6-fold less, $p < 0.0001$; Figure 4F) and by qPCR (10.1-fold less, $p = 0.0002$; Figures 5F and 5G). Moreover, although CRC colonization by the Fap2 expressing *F. nucleatum* ATCC 23726 strain is significantly higher than that of the adjacent normal colon ($p < 0.0001$ and $p = 0.0008$, Figures 4F and 4G, respectively), CRC colonization by D22 is not (Figures 5F and 5G). Co-challenge with ATCC 23726 and the other Fap2 mutant K50 co-injected into the CRC mouse model, confirm the involvement of Fap2 in CRC colonization by *F. nucleatum* ATCC 23726 (mean of competition index 25.5, $p = 0.0046$; Figure 5H). Using human colonic adenocarcinoma isolates, we found that the Fap2-expressing CTI-2 strain (Figure S1) is abundant in the tumors; however the Fap2-deficient CTI-7 strain is not detected in the tumors by plating (Figure 5I) and qPCR (Figure 5J). These results imply that although neoplastic tissues play a critical role in fusobacterial tumor enrichment, fusobacterial CRC-specific enrichment is also Fap2 dependent. These results also raise the question if there are excessive fitness costs to maintain Fap2 once *F. nucleatum* is established in a tumor, given Fap2's loss in the CTI-7 strain.

We next evaluated if fusobacteria could localize to CRC metastasis and whether this localization is Gal-GalNAc-Fap2 mediated. We detected *F. nucleatum* in human CRC metastases by qPCR (Figure 6A; 10 of 12 tested metastases), consistent with prior preliminary observations (Kostic et al., 2012), but we do not detect fusobacteria in 6 of 7 samples taken from tumor-free liver biopsies (Figure 6A). Interestingly, we found Gal-GalNAc expression in the 1 tumor-free liver sample (a fibrotic cyst) in which fusobacteria is detected (Figure S2). Presence of fusobacteria in CRC-metastasis colonization appears to be specific insofar as genomic DNA (gDNA) of *P. gingivalis* is not detected in the tested samples. Similar to primary colon adenocarcinoma, Gal-GalNAc is overexpressed (in comparison with adjacent normal tissue) in all of the tested metastases, from a variety of organs (Figures 6B and 6C). As we observed in CRC primary tumors, ex vivo binding of *F. nucleatum* ATCC 23726 to CRC metastases sections was Fap2 dependent, with reduced attachment of the Fap2-inactivated mutant K50 compared with wild-type (Figures 6D, 6E, and S3).

DISCUSSION

There is a growing interest in the role of bacteria in cancer biology and special interest in *F. nucleatum* in colorectal carcinogenesis. Although fusobacteria are found in CRC, to date, the mechanisms by which fusobacteria home and localize to colorectal tumors have been under-explored. Herein, using human CRC samples and an orthotopic mouse CRC model, we found that tumors and their metastases possess specific glycans that underlie fusobacterial tumor enrichment. Undoubtedly, other factors, such as tumor hypoxia and the tumor-immune microenvironment, contribute to a niche that allows for fusobacterial survival. However, these local environmental conditions were not sufficient to enable localization of another oral anaerobic bacterium, *P. gingivalis*, in CRC. Therefore, it seems that specific factors and mechanisms are required for CRC colonization by bacteria.

Binding between the fusobacterial adhesin FadA and host epithelial E-cadherin may enable fusobacterial attachment to CRC (Rubinstein et al., 2013). However, E-cadherin is expressed

on many cell types (Frixen et al., 1991; Heng and Painter, 2008), and its expression levels and cellular localization patterns in dysplasia and neoplasia can vary (Jiang et al., 2015; Schmalhofer et al., 2009). Thus its binding may not fully explain *F. nucleatum*'s tropism to CRC. Furthermore, not all human colon adenomas and adenocarcinomas express E-cadherin; nor do CT26 cells, which we used in our orthotopic CRC mouse model experiments (Grossi and Genco, 1998; Langlois et al., 2010). Thus our experiments support that additional mechanisms, specifically fusobacterial Fap2 and host Gal-GalNAc, are involved in fusobacterial CRC localization and enrichment.

Fap2 has multiple functions that may facilitate fusobacterial adaptation to different body habitats. In the oral cavity, Fap2 is mainly involved in attachment to neighboring bacteria (co-adherence) in a manner that bridges different species and increases the diversity and the stability of the developing dental plaque (Coppenhagen-Glazer et al., 2015; Kolenbrander and London, 1993). We also recently found that Fap2-deficient mutants are impaired in placental colonization (Coppenhagen-Glazer et al., 2015). In the colon, our data suggest that Fap2 mediates adenocarcinoma-specific binding through attachment to Gal-GalNAc, which we observed is expressed at high levels in CRC. Similar to CRC, the placenta has also been shown to overexpress Gal-GalNAc (Richter et al., 2000).

In tumors, we recently showed that Fap2 mediates fusobacterial-driven impairment of host anti-tumor immunity. Fap2 binds and activates TIGIT (Yu et al., 2009) an immunoregulatory signaling receptor in T cells and NK cells. This Fap2-TIGIT interaction reduces killing of tumor cells by NK and tumor-infiltrating lymphocytes (Gur et al., 2015). Fap2 has also been reported to induce lymphocyte apoptosis (Kaplan et al., 2005, 2010).

Although all of the oral isolates we examined herein expressed Fap2 and hemagglutinate, only three of the six CRC isolates are able to hemagglutinate (Figure S2). This may imply that Fap2-dependent attachment is selected for under the constant flow conditions of the oral cavity where surface attachment is vital; however, in tumors, after fusobacterial attachment and establishment in the adenocarcinoma niche, the selective pressure for Fap2 may be lost. In the future, it will be interesting to perform comparative genomic studies of fusobacterial isolates from the oral cavity, adenomas, adenocarcinomas, and metastatic sites in conjunction with host genomic profiling to understand the selective pressure that host tissue site exert on fusobacteria and that fusobacteria exert on host tissues.

In summary, our results unveil a host factor (Gal-GalNAc) and a microbial lectin (Fap2) that mediates fusobacterial enrichment in CRC in human tissues, human and mouse CRC cell lines, and a preclinical orthotopic CRC model as well as in human CRC metastases. Our findings support that targeting *F. nucleatum* Fap2 or host epithelial Gal-GalNAc expression may provide a means to block *F. nucleatum* potentiation of CRC and afford diagnostic opportunities as well.

EXPERIMENTAL PROCEDURES

Collection of Clinical Samples

The Hadassah Medical School institutional review board approved the use of human samples for this study. Informed consent was obtained from all patients. CRC metastases from five frozen and seven formalin-fixed paraffin-embedded blocks were collected from the Israel Collaborative Biorepository for Research (MIDGAM). Seven tumor-free liver tissue samples were collected from the pathology department at Hadassah Medical School.

Tissue Microarray Analysis

Colon cancer tissue array CO2601 (US Biomax) and array CO809a (US Biomax) were used in these studies. Details about the cases for each core on the array are available on the US Biomax Web site.

Bacterial Strains and Growth Conditions

F. nucleatum strains ATCC 23726, K50, D22, ATCC 10953, PK 1594, CTI-1, CTI-2, CTI-3, CTI-5, CTI-6, CTI-7, EAVG_002, and *P. gingivalis* ATCC 33277 were cultured as described in Supplemental Experimental Procedures. Regarding the use of the K50 and D22, two mutants strains derived from ATCC 23726 with a disrupted and inactive fap2 gene (Coppenhagen-Glazer et al., 2015), after Figure 2A, given the similarity in phenotype these strains are used interchangeably in subsequent experiments.

Cell Lines and Tissue Culture

CT26 stably transfected with the luciferase (*luc*) gene (CT26-luc), the human colon adenocarcinoma cell line HT29, RKO, and HCT116 were cultured according to ATCC guidelines. These cells were kind gifts from Professors Panet (CT26-luc), Ben-Neriah (HT29), Mandelboim (RKO), and Hoffman (HCT116).

Murine CRC Model

All experiments were performed in accordance with the guidelines of our institution's animal welfare committee. The orthotopic rectal cancer model was performed as described (Kolodkin-Gal et al., 2009) in wild-type BALB/cJ mice. Mice were injected with 1×10^6 CT26-luc cells. For tumor size assessment, see Supplemental Experimental Procedures.

Bacterial Inoculations

Mice were inoculated with 5×10^6 to 1×10^7 bacteria (washed with PBS twice) via tail vein injection. For C57BL/6J wild-type and $Apc^{Min+/-}$ mice, mice were aged beyond 12 weeks and then intravenously injected with ~5×10^8 prewashed bacteria.

Quantification of Bacteria Using Plating and qPCR

Tissue samples were homogenized using a Fastprep (MP Biomedicals) and plated as described in Supplemental Experimental Procedures. Colonies were enumerated after 6 days of incubation under anaerobic conditions. See Supplemental Experimental Procedures for details of DNA preparation and qPCR of homogenized tissue.

Flow Cytometry and Competition Assays

FITC-labeled *F. nucleatum* were incubated with cells at a MOI of 10 for 30 min at room temperature. FITC-labeled PNA lectin (Sigma-Aldrich) was incubated at a final concentration of 140 nM per 2.5×10^5 cells. For competition experiments, bacteria or PNA was incubated with GalNAc (concentration range 0, 50, 100, and 300 mM) for 30 min prior to incubation with cells. For flow cytometry methods and analysis, see Supplemental Experimental Procedures.

Immunofluorescence and Section Preparation

Fixed tissue sections were stained with H&E or processed for immunofluorescence microscopy as described below. Sections were blocked and incubated with fluorescent PNA or fluorescent bacteria as described in Supplemental Experimental Procedures. GalNAc removal was performed by incubating sections with O-glycanase; see Supplemental Experimental Procedures for experimental details. Imaging analysis is described in Supplemental Experimental Procedures.

Hemagglutination Assays

Hemagglutination assays were performed as previously described (Coppenhagen-Glazer et al., 2015). For inhibition assays, washed bacteria were preincubated with 25 mM GalNAc (Sigma-Aldrich) for 30 min prior to incubation with erythrocytes.

Statistical Analysis

GraphPad Prism software version 6.0 was used for statistical analysis. Statistical tests used are indicated in the figure legends.

Supplementary Material

Refer to Web version on PubMed Central for supplementary material.

Acknowledgments

We thank Professor Lawrence A. Tabak for useful discussions, Professor Norman Grover for valuable assistance in statistics, and Carey Ann Gallini for proofreading. This work was supported by the Israel Cancer Research Fund Project grant and Israel Science Foundation grant 201/15 to G.B. and grant RO1 CA154426 and a Hoffman-LaRoche research grant to W.S.G. W.S.G. is a SAB member of Evelo Therapeutics and Synlogic, has received research funds from Hoffman-LaRoche, and consults for Janssen Pharmaceuticals.

References

Arthur JC, Perez-Chanona E, Mühlbauer M, Tomkovich S, Uronis JM, Fan TJ, Campbell BJ, Abujamel T, Dogan B, Rogers AB, et al. Intestinal inflammation targets cancer-inducing activity of the microbiota. Science. 2012; 338:120–123. [PubMed: 22903521]

Ashare A, Stanford C, Hancock P, Stark D, Lilli K, Birrer E, Nymon A, Doerschug KC, Hunninghake GW. Chronic liver disease impairs bacterial clearance in a human model of induced bacteremia. Clin Transl Sci. 2009; 2:199–205. [PubMed: 20443893]

Belcheva A, Irrazabal T, Robertson SJ, Streutker C, Maughan H, Rubino S, Moriyama EH, Copeland JK, Kumar S, Green B, et al. Gut microbial metabolism drives transformation of MSH2-deficient colon epithelial cells. Cell. 2014; 158:288–299. [PubMed: 25036629]

Castellarin M, Warren RL, Freeman JD, Dreolini L, Krzywinski M, Strauss J, Barnes R, Watson P, Allen-Vercoe E, Moore RA, Holt RA. Fusobacterium nucleatum infection is prevalent in human colorectal carcinoma. Genome Res. 2012; 22:299–306. [PubMed: 22009989]

Chen W, Liu F, Ling Z, Tong X, Xiang C. Human intestinal lumen and mucosa-associated microbiota in patients with colorectal cancer. PLoS ONE. 2012; 7:e39743. [PubMed: 22761885]

Human Microbiome Project Consortium. Structure, function and diversity of the healthy human microbiome. Nature. 2012; 486:207–214. [PubMed: 22699609]

Coppenhagen-Glazer S, Sol A, Abed J, Naor R, Zhang X, Han YW, Bachrach G. Fap2 of Fusobacterium nucleatum is a galactose-inhibitable adhesin involved in coaggregation, cell adhesion, and preterm birth. Infect Immun. 2015; 83:1104–1113. [PubMed: 25561710]

Dewhirst FE, Chen T, Izard J, Paster BJ, Tanner AC, Yu WH, Lakshmanan A, Wade WG. The human oral microbiome. J Bacteriol. 2010; 192:5002–5017. [PubMed: 20656903]

Faust K, Sathirapongsasuti JF, Izard J, Segata N, Gevers D, Raes J, Huttenhower C. Microbial co-occurrence relationships in the human microbiome. PLoS Comput Biol. 2012; 8:e1002606. [PubMed: 22807668]

Flanagan L, Schmid J, Ebert M, Soucek P, Kunicka T, Liska V, Bruha J, Neary P, Dezeeuw N, Tommasino M, et al. Fusobacterium nucleatum associates with stages of colorectal neoplasia development, colorectal cancer and disease outcome. Eur J Clin Microbiol Infect Dis. 2014; 33:1381–1390. [PubMed: 24599709]

Frixen UH, Behrens J, Sachs M, Eberle G, Voss B, Warda A, Löchner D, Birchmeier W. E-cadherin-mediated cell-cell adhesion prevents invasiveness of human carcinoma cells. J Cell Biol. 1991; 113:173–185. [PubMed: 2007622]

Gao S, Li S, Ma Z, Liang S, Shan T, Zhang M, Zhu X, Zhang P, Liu G, Zhou F, et al. Presence of *Porphyromonas gingivalis* in esophagus and its association with the clinicopathological characteristics and survival in patients with esophageal cancer. Infect Agent Cancer. 2016; 11:3. [PubMed: 26788120]

Garrett WS. Cancer and the microbiota. Science. 2015; 348:80–86. [PubMed: 25838377]

Giannasca KT, Giannasca PJ, Neutra MR. Adherence of Salmonella typhimurium to Caco-2 cells: identification of a glycoconjugate receptor. Infect Immun. 1996; 64:135–145. [PubMed: 8557331]

Grossi SG, Genco RJ. Periodontal disease and diabetes mellitus: a two-way relationship. Ann Periodontol. 1998; 3:51–61. [PubMed: 9722690]

Gur C, Ibrahim Y, Isaacson B, Yamin R, Abed J, Gamliel M, Enk J, Bar-On Y, Stanietsky-Kaynan N, Coppenhagen-Glazer S, et al. Binding of the Fap2 protein of *Fusobacterium nucleatum* to human inhibitory receptor TIGIT protects tumors from immune cell attack. Immunity. 2015; 42:344–355. [PubMed: 25680274]

Hajishengallis G, Liang S, Payne MA, Hashim A, Jotwani R, Eskan MA, McIntosh ML, Alsam A, Kirkwood KL, Lambris JD, et al. Low-abundance biofilm species orchestrates inflammatory periodontal disease through the commensal microbiota and complement. Cell Host Microbe. 2011; 10:497–506. [PubMed: 22036469]

Han YW, Ikegami A, Rajanna C, Kawsar HI, Zhou Y, Li M, Sojar HT, Genco RJ, Kuramitsu HK, Deng CX. Identification and characterization of a novel adhesin unique to oral *fusobacteria*. J Bacteriol. 2005; 187:5330–5340. [PubMed: 16030227]

Heng TS, Painter MW, Immunological Genome Project Consortium. The Immunological Genome Project: networks of gene expression in immune cells. Nat Immunol. 2008; 9:1091–1094. [PubMed: 18800157]

Ito M, Kanno S, Nosho K, Sukawa Y, Mitsuhashi K, Kurihara H, Igarashi H, Takahashi T, Tachibana M, Takahashi H, et al. Association of *Fusobacterium nucleatum* with clinical and molecular features in colorectal serrated pathway. Int J Cancer. 2015; 137:1258–1268. [PubMed: 25703934]

Jiang WG, Sanders AJ, Katoh M, Ungefroren H, Gieseler F, Prince M, Thompson SK, Zollo M, Spano D, Dhawan P, et al. Tissue invasion and metastasis: molecular, biological and clinical perspectives. Semin Cancer Biol. 2015; 35(Suppl):S244–S275. [PubMed: 25865774]

Kaplan CW, Lux R, Huynh T, Jewett A, Shi W, Haake SK. Fusobacterium nucleatum apoptosis-inducing outer membrane protein. J Dent Res. 2005; 84:700–704. [PubMed: 16040725]

Kaplan CW, Ma X, Paranjpe A, Jewett A, Lux R, Kinder-Haake S, Shi W. Fusobacterium nucleatum outer membrane proteins Fap2 and RadD induce cell death in human lymphocytes. Infect Immun. 2010; 78:4773–4778. [PubMed: 20823215]

Katz J, Onate MD, Pauley KM, Bhattacharyya I, Cha S. Presence of Porphyromonas gingivalis in gingival squamous cell carcinoma. Int J Oral Sci. 2011; 3:209–215. [PubMed: 22010579]

Kolenbrander PE, Andersen RN. Inhibition of coaggregation between Fusobacterium nucleatum and Porphyromonas (Bacteroides) gingivalis by lactose and related sugars. Infect Immun. 1989; 57:3204–3209. [PubMed: 2777379]

Kolenbrander PE, London J. Adhere today, here tomorrow: oral bacterial adherence. J Bacteriol. 1993; 175:3247–3252. [PubMed: 8501028]

Kolodkin-Gal D, Edden Y, Hartshtark Z, Ilan L, Khalaileh A, Pikarsky AJ, Pikarsky E, Rabkin SD, Panet A, Zamir G. Herpes simplex virus delivery to orthotopic rectal carcinoma results in an efficient and selective antitumor effect. Gene Ther. 2009; 16:905–915. [PubMed: 19440231]

Kostic AD, Gevers D, Pedamallu CS, Michaud M, Duke F, Earl AM, Ojesina AI, Jung J, Bass AJ, Tabernero J, et al. Genomic analysis identifies association of Fusobacterium with colorectal carcinoma. Genome Res. 2012; 22:292–298. [PubMed: 22009990]

Kostic AD, Chun E, Robertson L, Glickman JN, Gallini CA, Michaud M, Clancy TE, Chung DC, Lochhead P, Hold GL, et al. Fusobacterium nucleatum potentiates intestinal tumorigenesis and modulates the tumor-immune microenvironment. Cell Host Microbe. 2013; 14:207–215. [PubMed: 23954159]

Langlois MJ, Bergeron S, Bernatchez G, Boudreau F, Saucier C, Perreault N, Carrier JC, Rivard N. The PTEN phosphatase controls intestinal epithelial cell polarity and barrier function: role in colorectal cancer progression. PLoS ONE. 2010; 5:e15742. [PubMed: 21203412]

McCoy AN, Araújo-Pérez F, Azcárate-Peril A, Yeh JJ, Sandler RS, Keku TO. *Fusobacterium* is associated with colorectal adenomas. PLoS ONE. 2013; 8:e53653. [PubMed: 23335968]

Mima K, Sukawa Y, Nishihara R, Qian ZR, Yamauchi M, Inamura K, Kim SA, Masuda A, Nowak JA, Nosho K, et al. Fusobacterium nucleatum and T cells in colorectal carcinoma. JAMA Oncol. 2015; 1:653–661. [PubMed: 26181352]

Mongiello JR, Falkler WA Jr. Sugar inhibition of oral Fusobacterium nucleatum haemagglutination and cell binding. Arch Oral Biol. 1979; 24:539–545. [PubMed: 44185]

Ozaki M, Miyake Y, Shirakawa M, Takemoto T, Okamoto H, Suginaka H. Binding specificity of Fusobacterium nucleatum to human erythrocytes, polymorphonuclear leukocytes, fibroblasts, and HeLa cells. J Periodontal Res. 1990; 25:129–134. [PubMed: 2141873]

Richter DU, Jeschke U, Makovitzky J, Goletz S, Karsten U, Briese V, Friese K. Expression of the Thomsen-Friedenreich (TF) antigen in the human placenta. Anticancer Res. 2000; 20(6D):5129–5133. [PubMed: 11326683]

Rubinstein MR, Wang X, Liu W, Hao Y, Cai G, Han YW. Fusobacterium nucleatum promotes colorectal carcinogenesis by modulating E-cadherin/Î2-catenin signaling via its FadA adhesin. Cell Host Microbe. 2013; 14:195–206. [PubMed: 23954158]

Sakuma S, Yu JY, Quang T, Hiwatari K, Kumagai H, Kao S, Holt A, Erskind J, McClure R, Siuta M, et al. Fluorescence-based endoscopic imaging of Thomsen-Friedenreich antigen to improve early detection of colorectal cancer. Int J Cancer. 2015; 136:1095–1103. [PubMed: 25052906]

Schmalhofer O, Brabletz S, Brabletz T. E-cadherin, beta-catenin, and ZEB1 in malignant progression of cancer. Cancer Metastasis Rev. 2009; 28:151–166. [PubMed: 19153669]

Sears CL, Garrett WS. Microbes, microbiota, and colon cancer. Cell Host Microbe. 2014; 15:317–328. [PubMed: 24629338]

Siegel RL, Miller KD, Jemal A. Cancer statistics, 2015. CA Cancer J Clin. 2015; 65:5–29. [PubMed: 25559415]

Springer GF. T and Tn, general carcinoma autoantigens. Science. 1984; 224:1198–1206. [PubMed: 6729450]

Strauss J, Kaplan GG, Beck PL, Rioux K, Panaccione R, Devinney R, Lynch T, Allen-Vercoe E. Invasive potential of gut mucosa-derived Fusobacterium nucleatum positively correlates with IBD status of the host. Inflamm Bowel Dis. 2011; 17:1971–1978. [PubMed: 21830275]

Tahara T, Yamamoto E, Suzuki H, Maruyama R, Chung W, Garriga J, Jelinek J, Yamano HO, Sugai T, An B, et al. Fusobacterium in colonic flora and molecular features of colorectal carcinoma. Cancer Res. 2014; 74:1311–1318. [PubMed: 24385213]

Thomas RM, Jobin C. The microbiome and cancer: is the “oncobiome” mirage real? Trends Cancer. 2015; 1:24–35. [PubMed: 26568984]

Tuttle RS, Strubel NA, Mourad J, Mangan DF. A non-lectin-like mechanism by which Fusobacterium nucleatum 10953 adheres to and activates human lymphocytes. Oral Microbiol Immunol. 1992; 7:78–83. [PubMed: 1528636]

Whitmore SE, Lamont RJ. Oral bacteria and cancer. PLoS Pathog. 2014; 10:e1003933. [PubMed: 24676390]

Wu S, Rhee KJ, Albesiano E, Rabizadeh S, Wu X, Yen HR, Huso DL, Brancati FL, Wick E, McAllister F, et al. A human colonic commensal promotes colon tumorigenesis via activation of T helper type 17 T cell responses. Nat Med. 2009; 15:1016–1022. [PubMed: 19701202]

Yang GY, Shamsuddin AM. Gal-GalNAc: a biomarker of colon carcinogenesis. Histol Histopathol. 1996; 11:801–806. [PubMed: 8839767]

Yu X, Harden K, Gonzalez LC, Francesco M, Chiang E, Irving B, Tom I, Ivelja S, Refino CJ, Clark H, et al. The surface protein TIGIT suppresses T cell activation by promoting the generation of mature immunoregulatory dendritic cells. Nat Immunol. 2009; 10:48–57. [PubMed: 19011627]

Highlights

- Gal-GalNAc is highly expressed in human CRC, metastases, and a preclinical CRC model
- Fap2 is a fusobacterial Gal-GalNAc-binding lectin
- Fap2 mediates *F. nucleatum* binding to Gal-GalNAc overexpressed in CRC
- Blood-borne Fap2-expressing *F. nucleatum* localizes to orthotopic mouse colon tumors

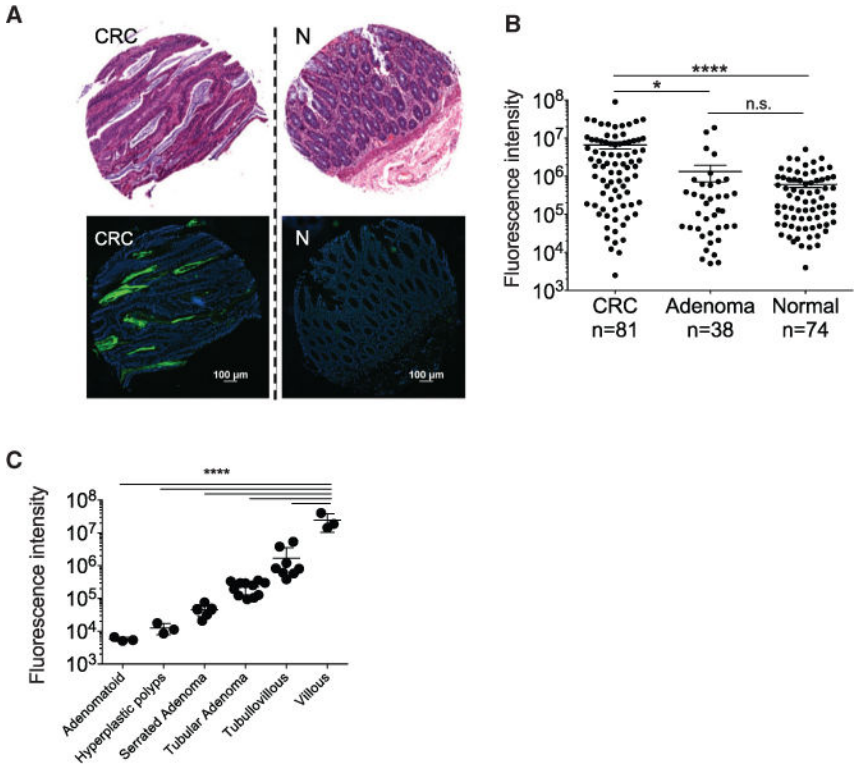

Figure 1. Gal-GalNAc Is Overexpressed in Human Colorectal Adenocarcinoma and Specific Adenoma Subgroups

(A and B) Gal-GalNAc levels in human colon adenocarcinomas, adenomas, and normal tissues using tissue microarrays (TMA). (A) Representative stained TMA images of human colon adenocarcinoma and normal tissue, H&E (top) and FITC-labeled Gal-GalNAc-specific PNA (green) and Hoechst dye (blue, bottom). (B) PNA binding to each tissue core (sum of fluorescence intensity of analyzed section; n, number of cases). Error bars indicate mean ± SEM. ****$p < 0.0001$, Wilcoxon signed-rank test.

(C) Gal-GalNAc expression within adenoma subgroups. PNA binding (sum of fluorescence intensity of analyzed section) to the adenoma tissue core presented in (B) and divided to adenoma groups. Error bars indicate mean ± SEM. ****$p < 0.0001$, ANOVA, Tukey's multiple comparison test.

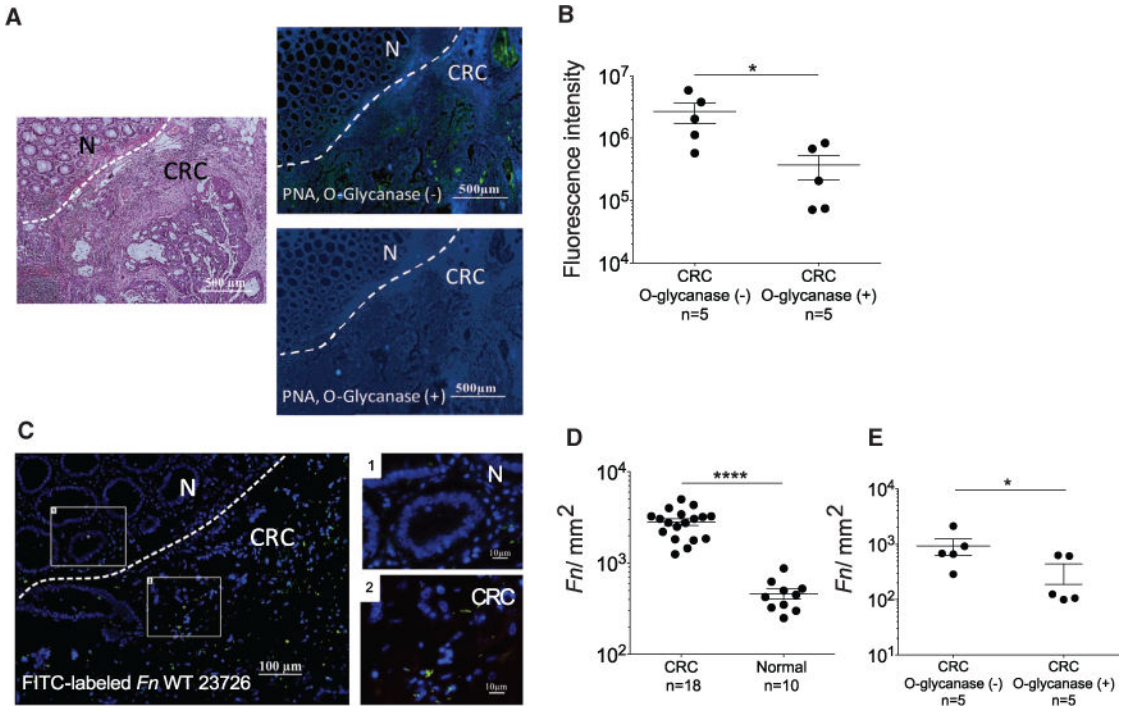

Figure 2. Gal-GalNAc Is Overexpressed in Human Colorectal Adenocarcinoma and Facilitates *F. nucleatum* Enrichment

(A) Human colon adenocarcinomas were treated with O-glycanase for Gal-GalNAc removal as indicated and stained as above. Dashed lines indicate CRC-adjacent normal tissue border.

(B) PNA binding (sum of fluorescence intensity of analyzed field) of samples untreated or treated with O-glycanase. Each symbol represents the mean of three randomly selected fields (n = 5 cases). Error bars indicate mean ± SEM. *p = 0.0313, Wilcoxon signed-rank test.

(C) Binding of FITC-labeled *Fn* (single green rods or aggregates seen as green spots) to Hoechst-stained (blue) human colon adenocarcinoma sections. Representative image (left) and magnified inset images (left).

(D) Quantitation of fusobacterial binding (*Fn*/mm^2) to TMA sections from human colon adenocarcinomas and normal tissues. Symbols represent individual cases. Error bars indicate mean ± SEM. ****p < 0.0001, one-tailed Mann-Whitney test.

(E) Quantitation of fusobacterial binding (*Fn*/mm^2) in CRC samples untreated or treated with O-glycanase. Each symbol represents the mean of three randomly selected fields per human section (n = 5 cases). Mean ± SEM are shown; *p = 0.0313, Wilcoxon signed-rank test.

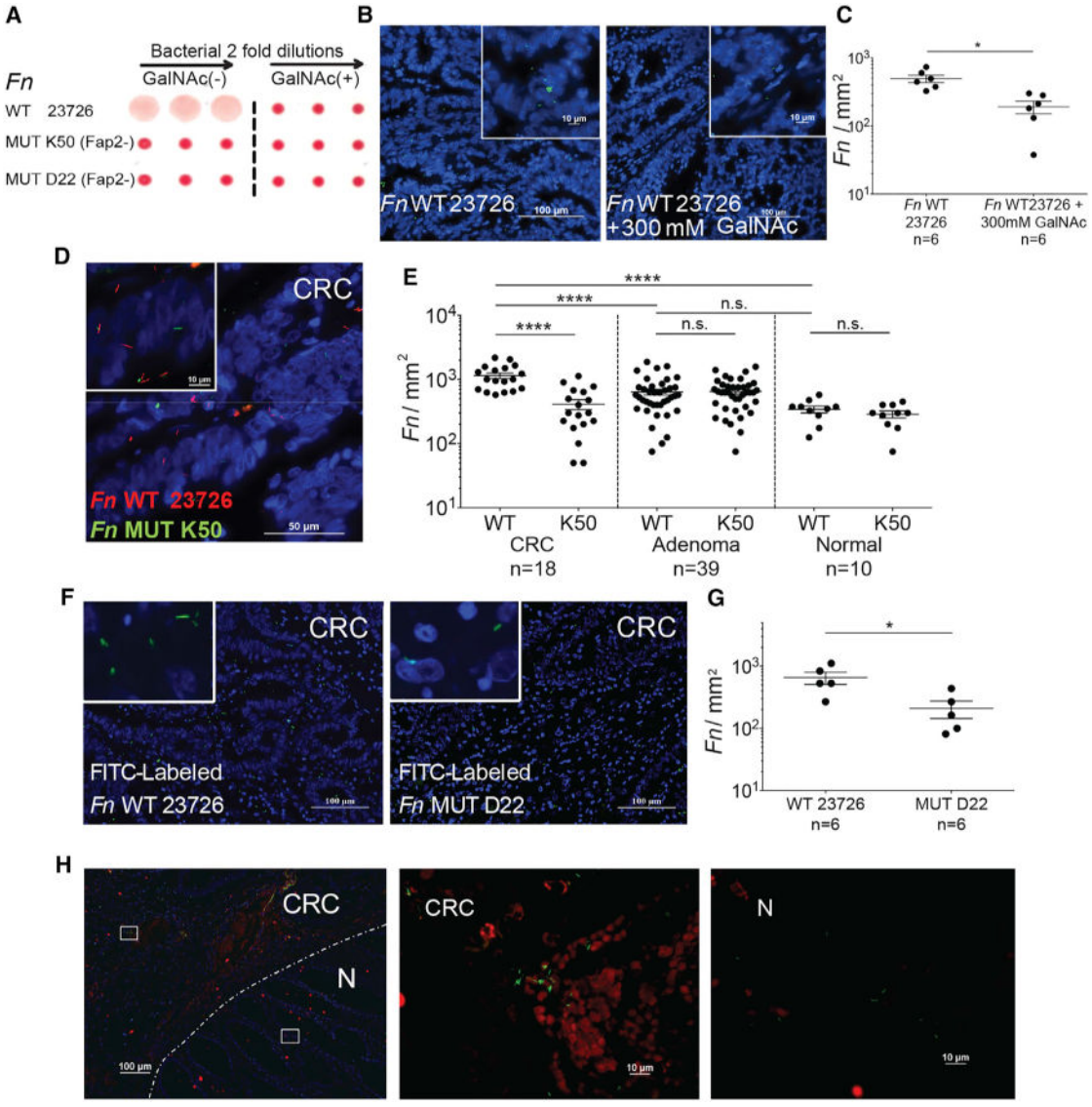

Figure 3. Fap2 Binding to GalNAc in Human CRC Mediates *F. nucleatum* Adenocarcinoma Enrichment

(A) Fap2 is a Gal-GalNAc binding lectin. Hemagglutination by wild-type *Fn* and not by isogenic Fap2 inactivated mutants K50 and D22 in the absence (left) and in the presence (right) of 25 mM GalNAc.

(B) Representative image of FITC-labeled *Fn* (green) attachment to Hoechst-stained (blue) human colon adenocarcinoma sections in the absence (left) or presence (right) 300 mM GalNAc.

(C) Quantitation of fusobacterial binding (*Fn*/mm^2) performed in (B). Each symbol represents the mean of three randomly selected fields per human section (n = 6). Mean ± SEM are shown; *p = 0.015, Wilcoxon signed-rank test.

(D) Representative image of Cy3-labeled *Fn* (red) and Cy5-labeled Fap2-inactivated isogenic mutant K50 (green) to a Hoechst-stained (blue) human colon adenocarcinoma section.

(E) Quantitation of fusobacterial binding (*Fn*/mm^2) to TMA of human colon adenocarcinoma, adenoma, and normal tissue. Each symbol represents the mean of three randomly selected fields per human tissue core. Mean ± SEM are shown; ****p < 0.0001, Bonferroni-corrected Wilcoxon test.

(F) Attachment of FITC-labeled (green) *Fn* (left) or of Fap2-inactivated isogenic mutant D22 (right) to Hoechst-stained (blue) representative human colon adenocarcinoma sections.

(G) Quantitation of fusobacterial binding (*Fn*/mm^2) described in (F). Each symbol represents the mean of three randomly selected fields per human section (n = 6). Mean ± SEM are shown; *p = 0.0119, one-tailed Mann-Whitney test.

(H) *Fn* colocalization with Gal-GalNAc in human CRC. Human colorectal adenocarcinoma sections were stained with Hoechst (blue) and incubated with Alexa Fluor 647-conjugated PNA (red) and FITC-labeled *Fn* (green). Dashed line indicates the CRC-adjacent normal tissue border. Representative image (left). Magnification of the inset CRC region is shown in the middle, and the inset adjacent to normal tissue is shown on the right.

See also Figure S1.

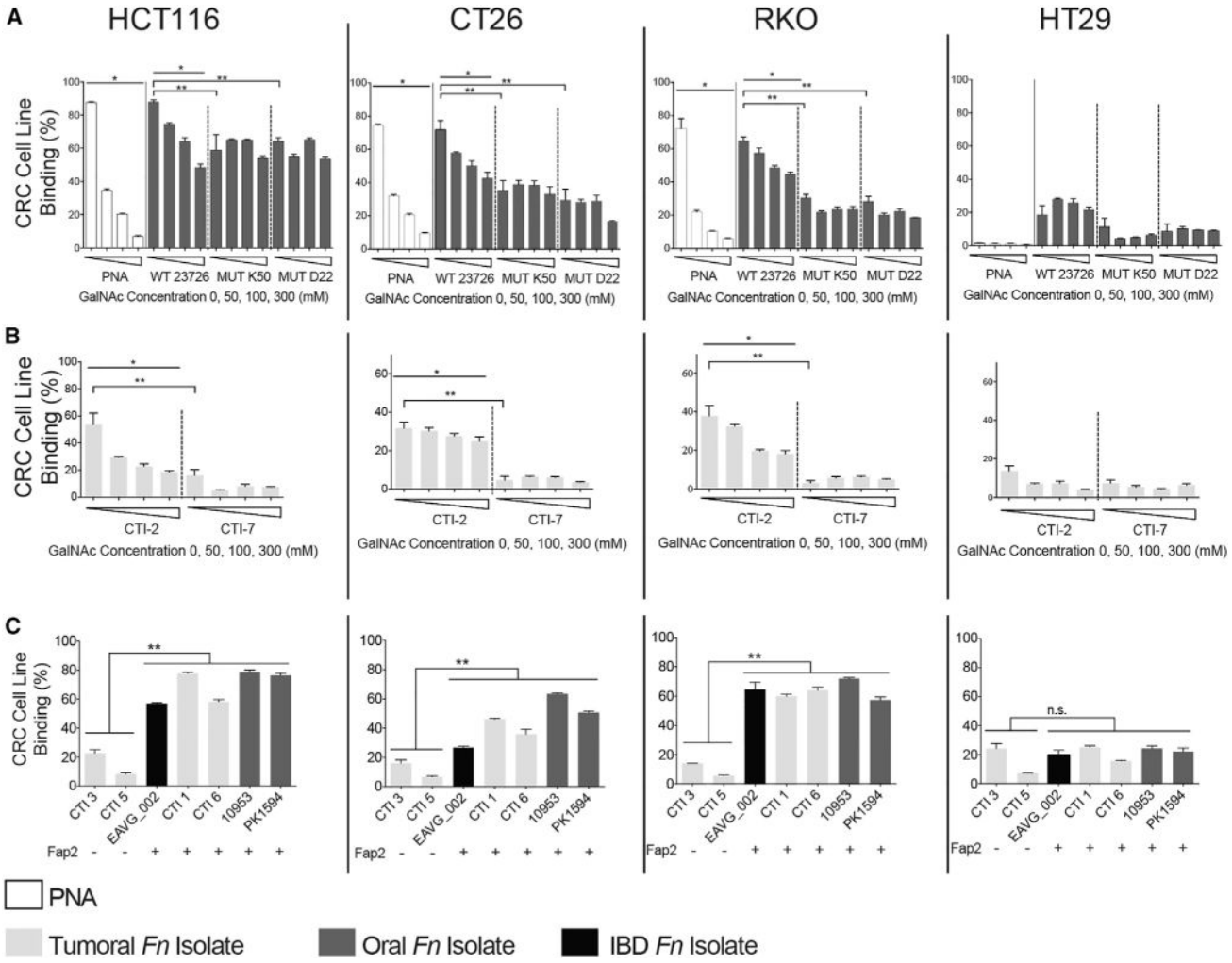

Figure 4. Fap2-Dependent Gal-GalNAc Binding Mediates *F. nucleatum* CRC Attachment

Flow cytometry analyses of attachments assays to mouse CRC cell line CT26 and human CRC cell lines HCT116, RKO, and HT29 without and with increasing concentrations of GalNAc.

(A) FITC-labeled PNA, *Fn*, Fap2-inactivated isogenic mutants K50 and D22.

(B) FITC-labeled human CRC *F. nucleatum* isolates CTI-2 and CTI-7.

(C) Binding of FITC-labeled *F. nucleatum* CRC isolates, oral isolates, and an inflammatory bowel disease isolate (as indicated) to mouse CRC cell line CT26 and human CRC cell lines HCT116, RKO, and HT29.

Data reflect three independent experiments. Mean values with SEM of triplicate are shown. Bacterial attachment data in the absence of GalNAc are the mean ± SEM of five independent experiments. *p = 0.04167, Spearman rank correlation coefficient; **p < 0.01, Bonferroni-corrected two-tailed Mann-Whitney test (**p < 0.01, ***p = 0.0007). See also Figure S1.

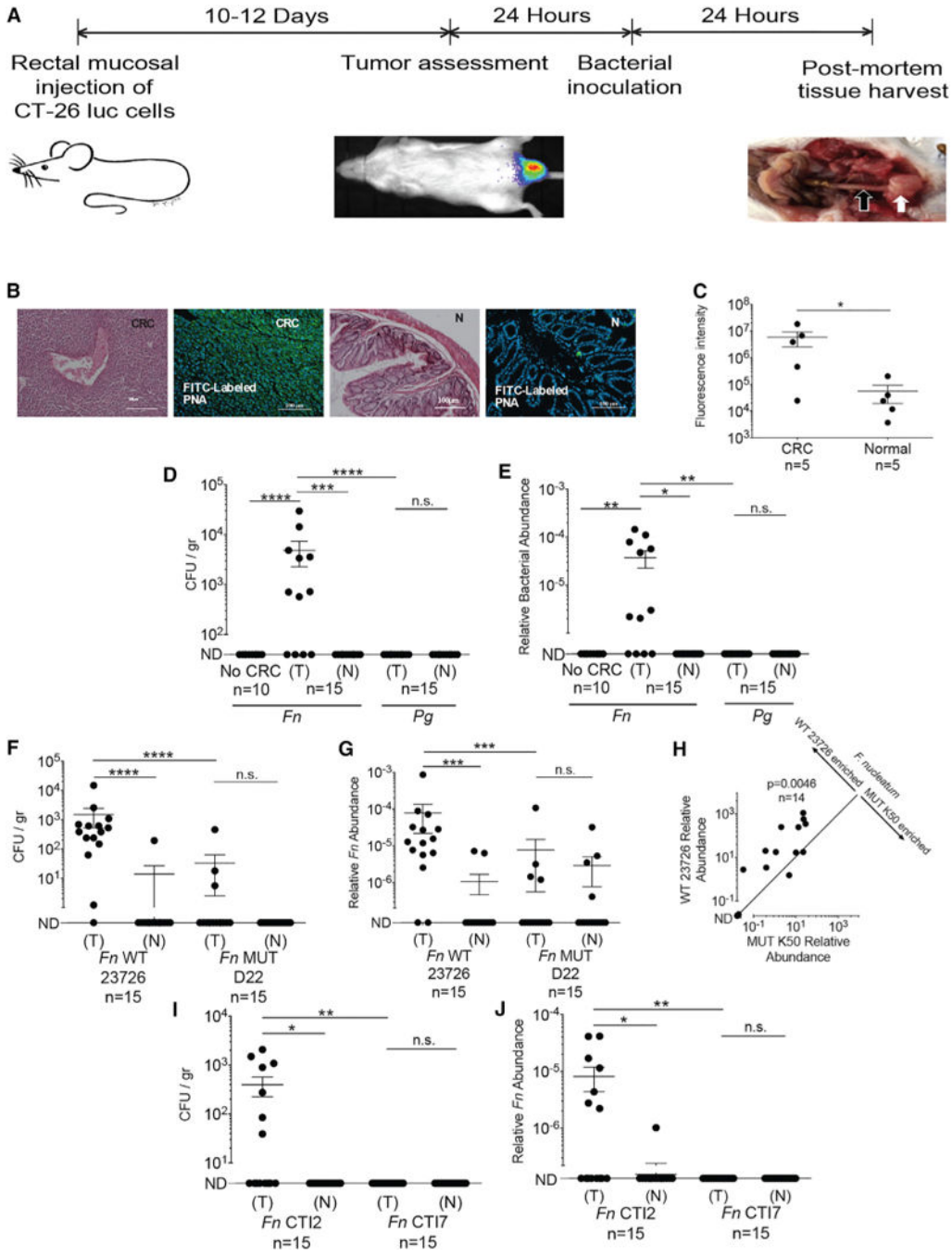

Figure 5. Localization of *F. nucleatum* to Established CRC Tumors Requires Fap2

(A) Experimental scheme: orthotopic rectal CT26 mouse CRC model. When tumors were 2,500 mm^3, mice were randomized to a bacterial inoculation group. White arrow indicates tumor, black arrow adjacent normal colon.

(B and C) Gal-GalNAc overexpression in the CT26 mouse CRC model. (B) Representative image of CT26 orthotopic tumor stained with H&E or with FITC-labeled Gal-GalNAc-specific PNA (green) and Hoechst dye (blue). CRC denotes images of tumors, and N denotes images of adjacent normal tissue. (C) Quantitative analysis of PNA binding to each

section (sum of fluorescence intensity of analyzed section). n, number of mice. Error bars indicate mean ± SEM. *p = 0.0313, Wilcoxon signed-rank test.

(D and E) Preferential enrichments of *F. nucleatum* ATCC 23726 in CRC tumors. (D) Abundance (CFU/gr tissue) and (E) relative fusobacterial gDNA abundance ($2^{-\Delta Ct}$) in colon samples from non-CT26 transplanted, tumor-free mice (no CRC), inoculated intravenously (IV) with 5×10^6 to 1×10^7 *F. nucleatum* ATCC 23726, in tumor (T) and normal adjacent tissues (N) from CT26-tumor-bearing mice (n = 15) inoculated IV with 5×10^6 to 1×10^7 *F. nucleatum* ATCC 23726 and in tumor (T) and normal adjacent tissues (N) from CT26-tumor-bearing mice (n = 15) inoculated IV with 5×10^6 to 1×10^7 *P. gingivalis* ATCC 33277 (*Pg*). ****p < 0.0001,**p < 0.01, Mann-Whitney U test; ***p = 0.0005, *p < 0.05, Bonferroni-corrected Wilcoxon signed-rank test. n.s., not statistically significant. Each symbol represents data from individual mice. Data reflect one representative experiment out of three performed in (B) and (C) and two in (D) and (E). Error bars show mean ± SEM.

(F–J) Fap2 mediates fusobacterial localization in CT26 CRC model mice. (F) CRC colonization (CFU/gr tissue) by IV inoculated *F. nucleatum* ATCC 23726 (*Fn* WT 23726) or Fap2-deficient mutant D22 (MUT D22). ****p < 0.0001, Bonferroni-corrected Wilcoxon signed-rank test for (T) versus (N); ****p < 0.0001, Mann-Whitney U test for (WT 23726) versus (MUT D22). (G) Relative fusobacterial gDNA abundance ($2^{-\Delta Ct}$) of wild-type *Fn* (WT) and of the Fap2-deficient isogenic mutant D22 in tumor (T) versus matched adjacent normal tissue (N) from the samples in (F). Error bars indicate mean ± SEM; ****p < 0.0001, ***p = 0.0002, Mann-Whitney U test.

(H) Tumor enrichment of *Fn* and the Fap2-deficient mutant K50 IV inoculated as a mixture; **p = 0.0046, Bonferroni-corrected Wilcoxon signed-rank test. (I and J) Tumoral enrichment of inoculated Fap2-expressing CTI-2 or of the Fap2-deficient CTI-7 in tumor (T) and normal tumor-adjacent tissues (N), quantified by plating (I) or by qPCR (J) as relative gDNA abundance in tumor versus matched adjacent normal tissue ($2^{-\Delta Ct}$); *p = 0.0156, **p = 0.0064, Bonferroni-corrected Mann-Whitney U test. Figures show data from one of two representative experiments performed.

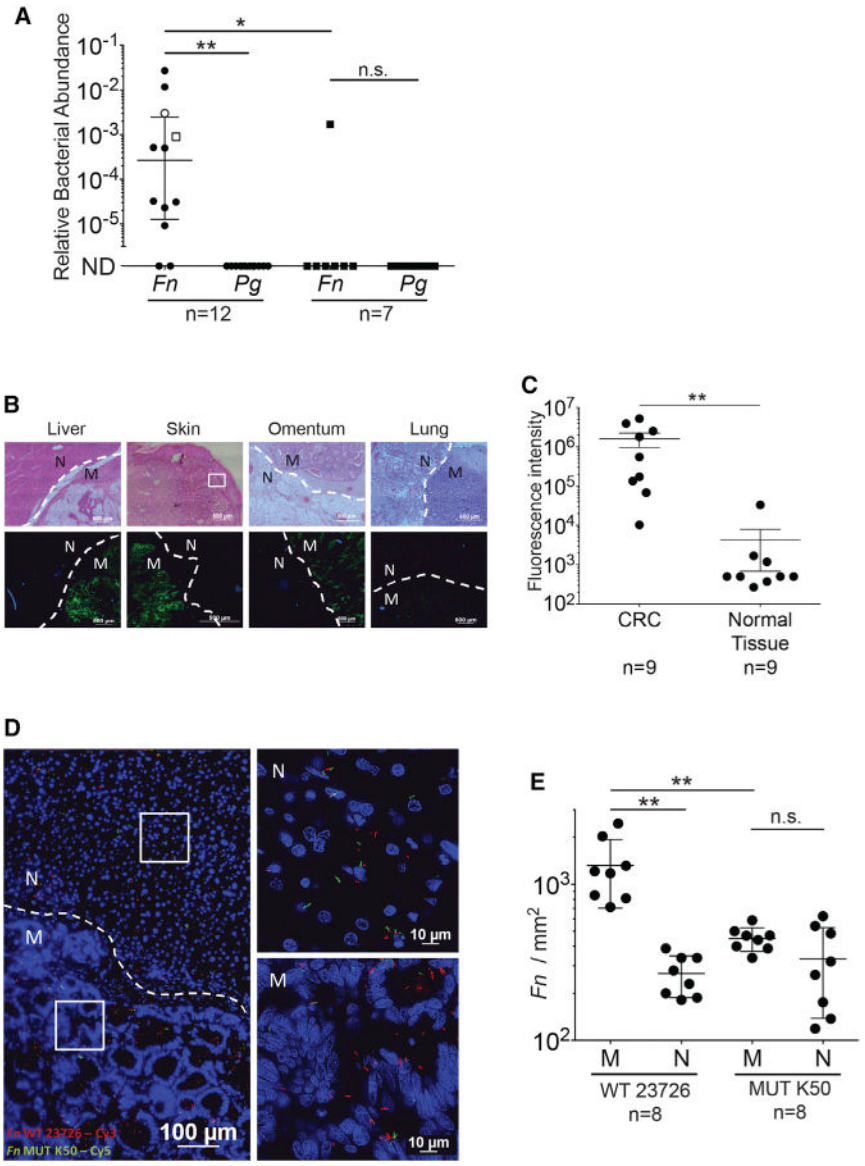

Figure 6. Fusobacterial Presence in CRC Metastases Is Facilitated by Fap2 Binding to Host Gal-GalNAc

(A) Relative fusobacterial (*Fn*) and *P. gingivalis* (*Pg*) gDNA abundance ($2^{-\Delta Ct}$) in human CRC metastases and in tumor-free liver biopsy samples. Open circle represents metastasis in the omentum, and open square represents metastasis in the lung. Filled circle are liver metastases. Filled squares represent tumor-free liver. Error bars indicate mean ± SEM; **p = 0.004, Bonferroni-corrected Wilcoxon signed-rank test; *p = 0.031, Bonferroni-corrected Mann-Whitney U test. Each symbol represents data from individual metastatic deposits.

(B) Representative sections of human CRC metastases (M) were stained with FITC-PNA (green) for Gal-GalNAc quantification and with Hoechst (blue). Dashed lines indicate tumor-adjacent normal (N) tissue border.

(C) Quantitative analysis of PNA binding (sum of fluorescence intensity of analyzed field) of the samples described in (B). Each symbol represents the mean of three randomly

selected fields for each human tissue section (n = 9). Error bars indicate mean ± SEM; **p = 0.0039, Wilcoxon signed-rank test.

(D) Attachment of Cy3-labeled (red) *Fn* and of its Cy5-labeled (green) Fap2-inactivated mutant K50 to a representative Hoechst-stained (blue) human CRC liver metastasis section. See Figure S4 for a representative section stained with Cy5-*Fn* and Cy3-K50, to allay concerns of dye staining bias.

(E) Quantitation of fusobacterial binding (Fn/mm^2) of bacteria described in (D) to sections of human CRC metastasis sections (n = 8). Each symbol represents the median of three randomly selected fields per human section. Error bars indicate mean ± SEM; **p = 0.0078, Wilcoxon signed-rank test.

See also Figures S2 and S3.